

Highly Reversible and Recyclable Absorption under Both Hydrophobic and Hydrophilic Conditions using a Reduced Bulk Graphene Oxide Material

Huicong Chang, Jili Qin, Peishuang Xiao, Yang Yang, Tengfei Zhang, Yanfeng Ma, Yi Huang, and Yongsheng Chen*

Materials with reversible and repeatable absorption for hydrophobicity and hydrophilicity conditions are highly needed for many different applications, such as large scale absorption for water or organic liquid,^[1,2] oil/water separation,^[3,4] and heavy-metal ions removal^[5] at harsh conditions for environmental-protection purposes, immobilization of proteins, and enzymes in biological^[6,7] and drug control release applications,^[8] and for liquid phase catalyst applications in both chemical and biological reactions.^[9,10] All these require the materials to have high structural and chemical stability. While many materials with repeatable absorption have been reported, most of them can only be applied for either hydrophobic or hydrophilic cases.^[11,12] For example, functionalized melamine sponge,^[13] nanofiber-assembled cellular aerogel,^[14–16] polymer aerogel,^[17,18] and carbonaceous materials^[11,19–21] have good absorption for organic absorbate at hydrophobic conditions because of their chemical nature and can be widely used for water purification. Nevertheless, these materials cannot be switched to absorb water at hydrophilic conditions.^[22] Even though external stimulus, such as pH,^[23] temperature,^[24] and light,^[25] was used to reversibly switch material's wettability between hydrophobicity and hydrophilicity, these materials were either film or coated on substrate that cannot absorb liquid largely to be applied in bulk, either under hydrophobic or hydrophilic conditions. To our knowledge, no material so far has been reported for reversible, recyclable, and large-scale absorption, in both cases of hydrophobic and hydrophilic environments.

Graphene materials have been reported for many absorption applications in both hydrophobic and hydrophilic environments

due to its high surface area, excellent mechanical performance, and easily controllable surface property (wettability).^[26–31] Some have shown extremely large absorption capacity for organic absorbate up to ≈ 1000 times of its weight in vacuum, but with limited repeating cycles.^[28] Though switchable surface wettability of supported graphene film or aerogel materials between hydrophobic and hydrophilic have been reported,^[29,32,33] these materials do not exhibit reversible and repeatable absorption between hydrophobic and hydrophilic conditions. Recently, we have developed a 3D crosslinked reduced graphene oxide material (3DG), which exhibits a super-absorption capacity for various hydrophobic liquids due to its high porosity and outstanding mechanical performance.^[34] Excitingly, this material also exhibits highly reversible compression cycles with Poisson's ratio near zero, so it would be very desirable if this material can demonstrate reversibly repeatable absorption for both hydrophobic and hydrophilic cases.

Herein, using this 3DG material, we have demonstrated a simple method to achieve such a switchable wettability between hydrophobicity (lipophilicity) and hydrophilicity. As shown in **Figure 1**, with ozone (O_3) treatment of the initial hydrophobic material (hydrophobic state), the obtained material could be turned to be hydrophilic. Then, with a simple annealing treatment of the obtained hydrophilic material (hydrophilic state) under an inert atmosphere, the hydrophobic property could be recovered again. Furthermore, a highly repeatable and reversible absorption with hundreds of compressing-releasing cycles was demonstrated both under hydrophobic and hydrophilic conditions.

The material was prepared through a solvothermal method described in our previous work (details are provided in the Experimental Section),^[34] exhibiting a near air density, 99.9% porosity, and super-compressive elasticity with oil contact angle (OCA) of $55.4^\circ \pm 0.9^\circ$ for petroleum ether and water contact angle (WCA) of $118.0^\circ \pm 1.8^\circ$ (Figure S1a,b, Supporting Information) measured using the captive bubble method and thus exhibiting a strong hydrophobicity as reported before. Its hydrophobic absorption with high capability for various organic liquids, compared with other reported materials, is shown in **Figure 2a**. Note that though the material exhibits some water absorption, the capacity is much smaller than the absorption capacity for organic liquids. For all the tested organic liquids, the material has higher absorption capacity than other materials. Note that no leaking was observed for the absorption.^[34] Importantly, such excellent absorption was also highly repeatable with retained $\approx 100\%$ capability during the

H. Chang, J. Qin, P. Xiao, Y. Yang, Dr. T. Zhang,
Prof. Y. Ma, Prof. Y. Huang, Prof. Y. Chen
Centre for Nanoscale Science and Technology
Collaborative Innovation Center of Chemical
Science and Engineering (Tianjin)
School of Materials Science and Engineering
Nankai University
Tianjin 300071, China
E-mail: yschen99@nankai.edu.cn



H. Chang, J. Qin, P. Xiao, Y. Yang, Dr. T. Zhang, Prof. Y. Ma,
Prof. Y. Huang, Prof. Y. Chen
State Key Laboratory and Institute of Elemento-Organic Chemistry
Institute of Polymer Chemistry
College of Chemistry
Nankai University
Tianjin 300071, China

DOI: 10.1002/adma.201505420

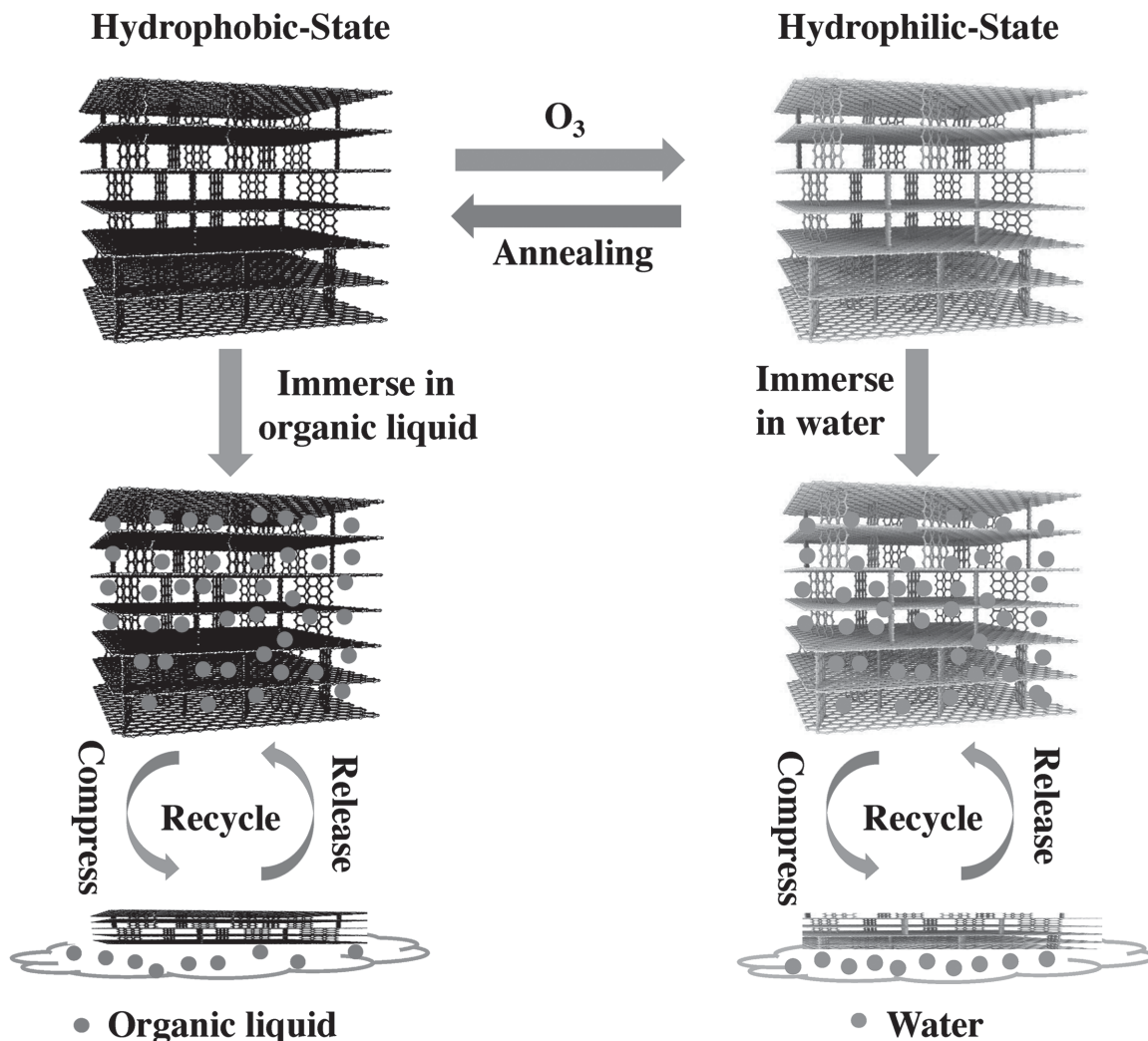


Figure 1. The diagram of switching wettability of the 3DG between hydrophobicity and hydrophilicity for reversible absorption. Under O_3 treatment of the initial hydrophobic-state material, the obtained material turned to be superhydrophilic. Furthermore, with annealing of the obtained hydrophilic-state material, the hydrophobic property could be recovered again. And a highly repeatable and reversible absorption under compressing–releasing cycles was demonstrated both in hydrophobic and hydrophilic conditions.

tested 200 compression cycles for various organic liquids, as shown in Figure 2b, and Figure S2 and Table S1 (Supporting Information). Such an outstanding and repeatable absorption ability was attributed to its extremely low density, high porosity, close to 100%, together with its well-kept entire structure integrity due to the existing 3D crosslinked bonding between the graphene sheets.^[34] Furthermore, the material presents a high absorption efficiency. When the saturated material was compressed, the absorbed liquid was squeezed out almost completely, and the material can be reused without any damage again for absorption–releasing cycle (Figure 1). This is due to its well-kept structural integrity mentioned above,^[34] which will be discussed below.

With such highly repeatable absorption at $\approx 100\%$ retained efficiency for hydrophobic systems, it would be very desirable if such high repeatable absorption could be switchable between hydrophobic and hydrophilic systems. Thus, considering the unique structure of this material and the chemistry

of graphene, a simple O_3 and annealing treatment was used to switch its wettability between hydrophobicity and hydrophilicity, as shown in **Figure 3a** for such a case with a reversible absorption process between water and petroleum ether. More experimental details and observations are shown in Video S1 and S2 (Supporting Information). After O_3 treatment to the initial hydrophobic-state material, the obtained hydrophilic-state material exhibits excellent water wettability and the absorption capacity for water reaches 870 times its weight with a WCA of $41.3^\circ \pm 3.2^\circ$ (Figure S1c, Supporting Information), compared with that ($118^\circ \pm 1.8^\circ$) before the treatment, though it still demonstrates some wetting for organic liquid with OCA of $63.8^\circ \pm 2.4^\circ$ for petroleum ether (Figure S1d, Supporting Information) and the corresponding absorption capacity is much smaller than that of the water absorption. The above results of contact angles were measured using the more reliable captive bubble method because it is difficult to measure the contact angle using the normal

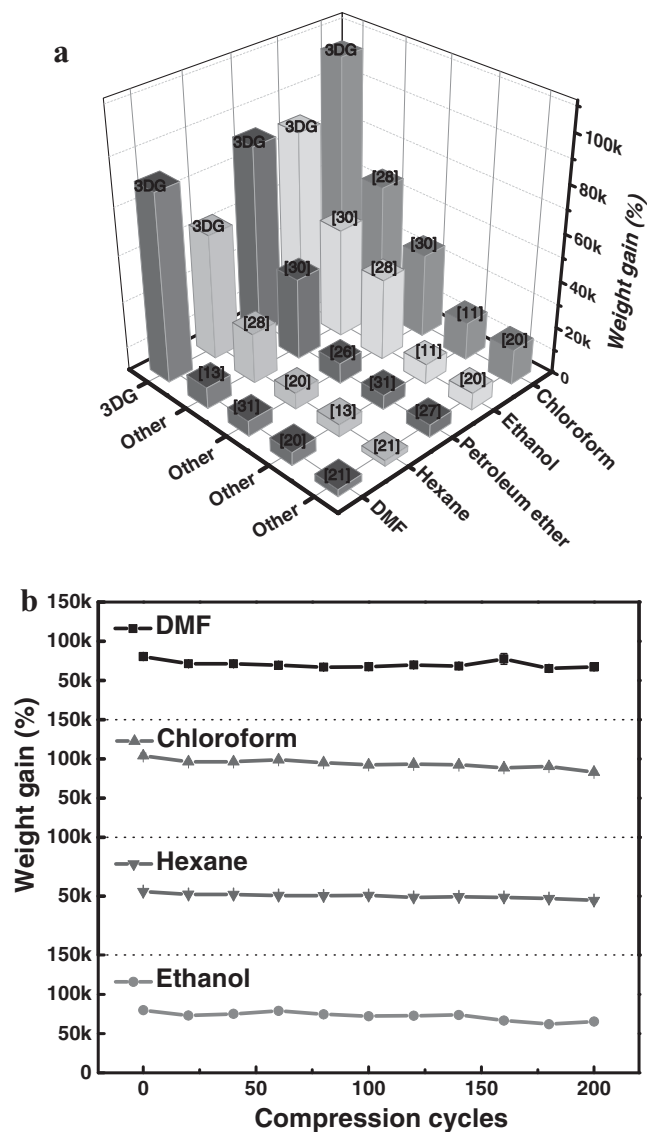


Figure 2. a) Comparison of absorption capacity for various organic liquids of the initial hydrophobic-state 3DG with other reported materials.^[11,13,20,21,26–28,30,31] It showed that the material could absorb 697, 600, 821, 800, and 1050 times of its weight for DMF, hexane, petroleum ether, ethanol, and chloroform, respectively. It exhibited much higher absorption capacity for any organic liquid than reference materials. b) The absorption capacity of the hydrophobic-state material versus the compression cycles in ethanol, hexane, chloroform, and DMF, respectively. The material showed high recyclability with $\approx 100\%$ retained absorption capacity.

sessile drop method due to the strong capillary effect caused by its highly porous structure ($>99.9\%$ porosity) (Table S2, Supporting Information). Again, when the water-saturated hydrophilic-state material was compressed, the absorbed water was mostly squeezed out, and then when it is immersed in water again, it could recover fully to its original volume with same saturation (Figure 3a; Video S1, Supporting Information). Same as the initial hydrophobic-state material, the newly hydrophilic-state material exhibits a repeatable high absorption capacity with excellent recyclability in water (Figure 3b). The compression stress versus the loss of the absorbed liquid was

measured for the *N,N*-dimethylformamide (DMF)-saturated hydrophobic-state material and water-saturated hydrophilic-state material (Figure S3, Supporting Information), indicating higher compression/strain squeezes out more liquid. Again, the reversible process (the switch between hydrophobicity and hydrophilicity) for the initial hydrophobic-state material can be achieved even after 30 times of repeating absorption releasing for water (Figure 3c–e).

More remarkably, the O_3 treatment generated hydrophilic-state material could be switched back to be hydrophobic by a simple annealing treatment under inert atmosphere, demonstrated with its OCA for petroleum ether of $52.4^\circ \pm 3.2^\circ$ and WCA of $115.8^\circ \pm 2.1^\circ$ (Figure S1e,f, Supporting Information), similar as the initial hydrophobic-state material. The structural recovery from hydrophilic state to hydrophobic state was also demonstrated by the recovered I_D/I_G from the Raman spectrum (Figure S4, Supporting Information). More importantly, its high and repeatable organic liquid absorption capacity and recyclability was also recovered as shown in Figure 3c–e, comparable with that for the initial hydrophobic-state material (Figure 2b). Strikingly, such reversible process, two way conversion between hydrophobicity and hydrophilicity could be repeated at least three times and the materials at each state all demonstrated similar high absorption for both organic liquids and water with high retained efficiency (Figure S5, Supporting Information).

We argue that the excellent reversibility and recyclability performance of this 3DG bulk material was due to its unique and stable structure and morphology as reported before,^[34] where 3D crosslinked graphene sheets were found, together with the intrinsic superior mechanical properties of graphene and its high stability. Furthermore, no visible damage of the microstructure was observed in the reversible process and the compression cycles from the scanning electron microscopy (SEM) results (Figure S6a–c, Supporting Information).

We argue that this material's switchable absorption capability between hydrophobicity and hydrophilicity was mainly induced by the surface chemical composition change as supported below by the chemical composition analysis due to the oxygen-containing group change, though it has been pointed that the absorption/desorption due to airborne contaminants has great impact on graphene's intrinsic WCA. When the initial hydrophobic-state material was treated with O_3 , due to its high surface area and near 100% porosity, ozone molecules could quickly enter the internal of the sample and react with graphene sheet to produce significant oxygen-containing groups, such as hydroxy, lactol, ester, and ketone groups, on its surface and edge as has been well demonstrated widely before (Figure 4).^[35–37] These groups could form abundant hydrogen bonds with water molecules very quickly once the material contacted with water. Also, as has been indicated earlier,^[32] the possible hydrocarbon contaminants absorbed on the material surface should be removed mostly, which would also improve its water wettability in some extent. With the synergic effect of the enhanced intrinsic wetting property for water and the capillary effect^[38] resulted from the porous surface topography characterized by SEM (Figure S6d,e, Supporting Information), and also possibility from the contribution of the removal of the surface hydrocarbon contaminants from air, the water molecules could quickly spread from the surface of the material to its internal

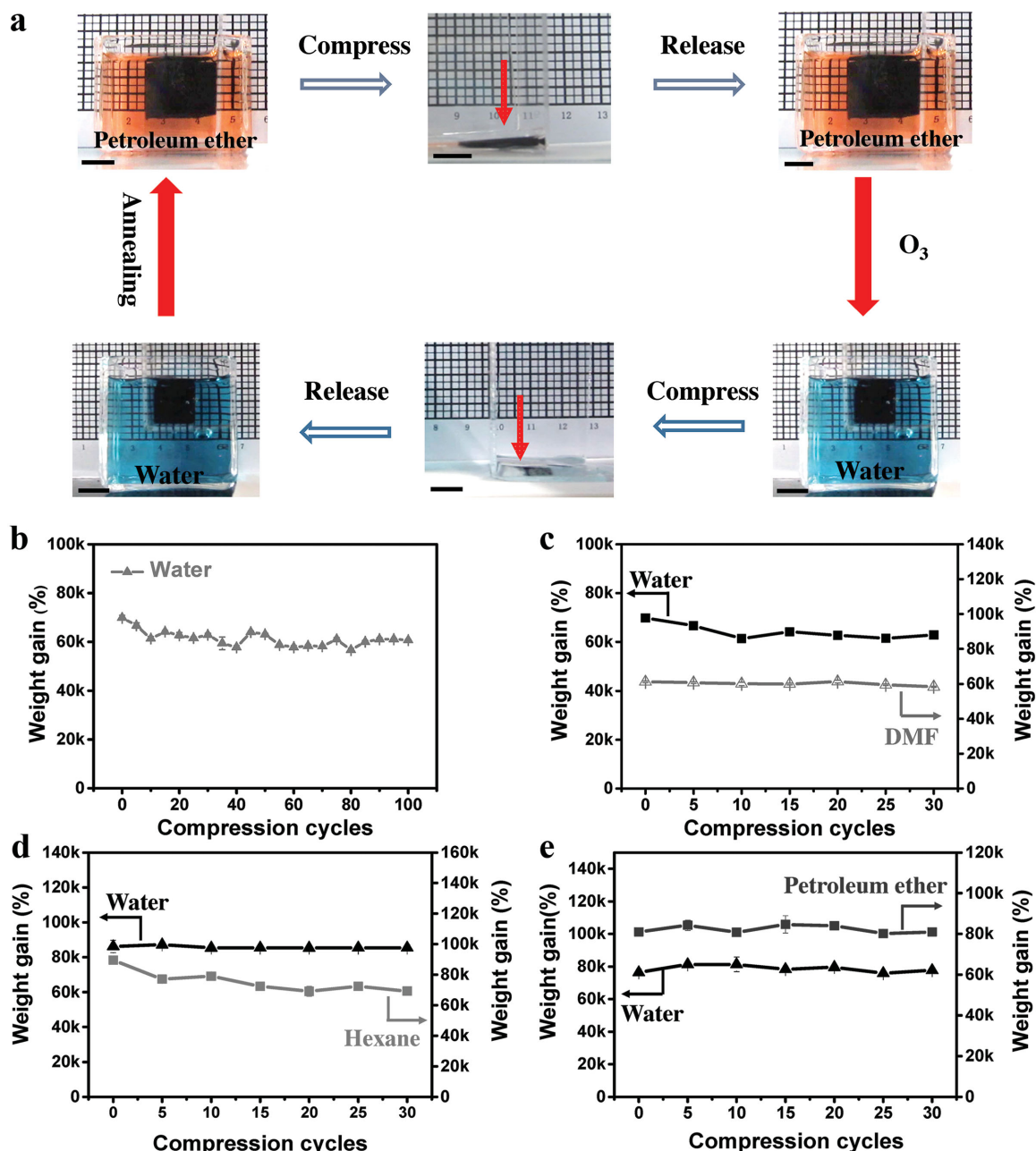


Figure 3. a) Photographs of the reversible absorption process between water and petroleum ether. Both in water and petroleum ether, when the absorbed liquid was squeezed out, the sample recovered its original volume quickly once immersed in the liquid again. Scale bars, 1 cm. For easy observation, the water was stained with bromocresol green and the petroleum ether was stained with Sudan III. b) The absorption capacity for water versus compression cycles of hydrophilic-state material obtained by O_3 treatment. c–e) The absorption capacity versus compression cycles of the hydrophilic-state material obtained by O_3 treatment for water and the regenerated hydrophobic-state material obtained by further annealing for c) DMF, d) hexane, and e) petroleum ether in a reversible process.

pores (Figure 4) totally, thus a clear water wetting performance was observed for the O_3 -treated material. Then, the following annealing could remove such added oxygen-containing groups without damaging its main structure and thus the structure integrity was kept. Note clearly, the impact of the likely airborne contaminants could not be ruled out, as this could be a very complicated issue and need much studies under rather strictly controlled environment also using well-controlled sample for

a reliable conclusion.^[32] Such a surface functionality switch in the reversible process has been supported by the elementary analysis (EA) (Table S3, Supporting Information) and the X-ray photoelectron spectrum (XPS) (Table S4 and Figure S7a,b and S8, Supporting Information) results. The oxygen content of the fresh material after O_3 treatment increased by ≈ 6.64 wt% from EA and 9.27 wt% from XPS, from hydrophobic state to hydrophilic state. Note, the above results were all obtained using

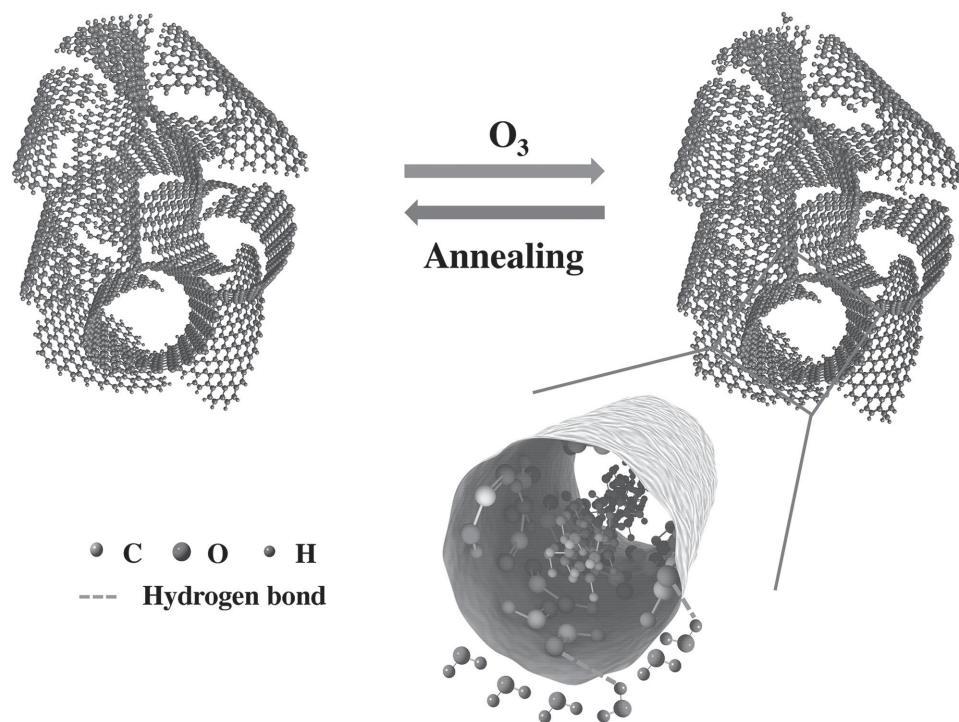


Figure 4. The reversible surface chemical composition change of the graphene sheets in the 3DG. When the initial hydrophobic-state material was treated with O_3 , ozone molecules quickly entered into the internal of the material and reacted with graphene sheet to produce lots of oxygen-containing groups on its surface and edge, which made the material superhydrophilic. With the synergic effect of the wetting for water and the capillary effect, water would quickly spread from the surface to internal pores. Furthermore, with the annealing treatment of the obtained hydrophilic-state material, the oxygen-containing groups were mostly removed and the material turned to be hydrophobic again.

the fresh material after O_3 treatment. Further XPS analysis indicates that the oxygen-containing groups on the surface of the O_3 -treated sample (hydrophilic-state material) decreased slowly due to their slow decomposing/cleavage along with time (Figure S9a, Supporting Information), the corresponding time-dependent study for contact angle (CA) and absorption for the O_3 -treated sample (Figure S9b–d, Supporting Information). Based on these results, we argue that such abundant oxygen-containing groups, though the likely surface airborne contamination might have a role too, have changed their surface wetting property from hydrophobicity to hydrophilicity as also demonstrated in the WCA (Figure S1c, Supporting Information). Furthermore, such surface chemical change seems to have smaller impact on the OCA due to the well-kept overall topography and morphology (Figure S1, Supporting Information). Obviously, the exact mechanism behind the wetting performance needs further studies under strict environments when considering the likely surface airborne contamination.^[32]

In conclusion, a bulk 3DG material with switchable capability between hydrophobicity and hydrophilicity has been demonstrated with high and repeatable absorption in both hydrophobic and hydrophilic environments, achieved by a simple O_3 and annealing treatment. The well-retained and repeatable absorption during the wetting switchable process is due to its unique structure of this bulk material, together with the intrinsic properties of graphene. During each of the O_3 and annealing treatment, the entire structure integrity and thus its super elasticity were retained, including its near 100% porosity. This excellent and reversible absorption

performance might make the graphene material highly promising for large-scale and reversible absorption under both hydrophobic and hydrophilic environments, under even harsh conditions, due to the chemical nature of graphene and carbon.

Experimental Section

Synthesis of 3DG: The material was prepared as following procedures. The starting material, graphene oxide (GO), was synthesized by the oxidation of natural graphite powder using a modified Hummers' method based on references in work by Chen et al.^[39] 3DG was prepared following our previous procedures.^[34] A low-concentration GO ethanol solution ($\approx 0.5 \text{ mg mL}^{-1}$) was solvothermally treated in a Teflon-lined autoclave at 180°C for 12 h. Then the as-prepared ethanol-filled intermediate product was carefully removed from the autoclave to have a slow and gradually solvent exchange with water. After the solvent exchange process was totally completed, the water-filled product was freeze dried. Finally, the material was annealed at 800°C for an hour in argon atmosphere to obtain the 3DG. The densities of the 3DG were $0.5\text{--}2.0 \text{ mg cm}^{-3}$. The carbon and oxygen element analysis results of samples were shown in Table S3–S5 (Supporting Information) obtained from XPS and EA.

Switching between Hydrophilic State and Hydrophobic State: The initial hydrophobic graphene material (hydrophobic state) was obtained by cutting the 3DG into about $10 \text{ mm} \times 10 \text{ mm} \times 10 \text{ mm}$ cuboid by laser. To switch the material to hydrophilic state, the above hydrophobic-state material was treated in a UV ozone system for 15 min. To again switch back to the hydrophobic state for the O_3 -treated material, the hydrophilic-state material was first dried using dry freezing and then annealed at 800°C under argon atmosphere for 1 h to obtain the regenerated hydrophobic-state material.

Cycling Test for Absorption: The recyclability measurement of the samples for both water and organic liquid absorption/releasing was carried out as follows: The hydrophilic-state/hydrophobic-state material was first immersed in the desired liquid and fully saturated, and then it was taken out carefully and weighted. Then the absorbed liquid was squeezed out by full compression the material. Finally, the fully compressed material was put into the liquid again to repeat the cycling test. In the cyclic process, the liquid absorbed sample was weighted by a balance with 0.01 mg precision. Weight gain was calculated by following formula: $\frac{m_1 - m_0}{m_0} \%$, where m_0 is the weight of the dry sample without absorption liquid and m_1 is the total weight of the sample and the absorbed liquid.

Compress Stress Measurement of Samples Saturated with Liquid: The sample first fully absorbed liquid and was put on the balance. Then it was compressed slowly to a certain strain at a constant strain rate (10% strain s^{-1}). The stress (compress force) was recorded with the balance reading directly. Then, after absorbing the liquid squeezed out with the filter paper and removing the compress force, the amount of the liquid squeezed out was obtained by the weight difference.

Supporting Information

Supporting Information is available from the Wiley Online Library or from the author.

Acknowledgements

The authors gratefully acknowledge financial support from the Ministry of Science and Technology of China (MoST) (Grant No. 2012CB933401) and the National Natural Science Foundation of China (NSFC) (Grant Nos. 91433101, 21374050, and 51273093).

Received: November 3, 2015

Revised: January 24, 2016

Published online: March 1, 2016

- [1] P. Kùsgens, M. Rose, I. Senkovska, H. Fröde, A. Henschel, S. Siegle, S. Kaskel, *Microporous Mesoporous Mater.* **2009**, *120*, 325.
- [2] S. Henninger, F. Schmidt, H.-M. Henning, *Appl. Therm. Eng.* **2010**, *30*, 1692.
- [3] B. Xin, J. Hao, *Chem. Soc. Rev.* **2010**, *39*, 769.
- [4] M. A. Shannon, P. W. Bohn, M. Elimelech, J. G. Georgiadis, B. J. Marinas, A. M. Mayes, *Nature* **2008**, *452*, 301.
- [5] J. S. Hu, L. S. Zhong, W. G. Song, L. J. Wan, *Adv. Mater.* **2008**, *20*, 2977.
- [6] M. Park, S. S. Park, M. Selvaraj, D. Zhao, C.-S. Ha, *Microporous Mesoporous Mater.* **2009**, *124*, 76.
- [7] M. Hartmann, *Chem. Mater.* **2005**, *17*, 4577.
- [8] H. Shen, L. M. Zhang, M. Liu, Z. J. Zhang, *Theranostics* **2012**, *2*, 283.
- [9] L. Liu, Y. P. Zhu, M. Su, Z. Y. Yuan, *ChemCatChem* **2015**, *7*, 2765.
- [10] D. Brunel, A. C. Blanc, A. Galarneau, F. Fajula, *Catal. Today* **2002**, *73*, 139.
- [11] B. Chen, Q. Ma, C. Tan, T. T. Lim, L. Huang, H. Zhang, *Small* **2015**, *11*, 3319.
- [12] B. Wang, W. Liang, Z. Guo, W. Liu, *Chem. Soc. Rev.* **2015**, *44*, 336.
- [13] D. D. Nguyen, N.-H. Tai, S.-B. Lee, W.-S. Kuo, *Energy Environ. Sci.* **2012**, *5*, 7908.
- [14] Y. Si, Q. Fu, X. Wang, J. Zhu, J. Yu, G. Sun, B. Ding, *ACS Nano* **2015**, *9*, 3791.
- [15] H. Bi, Z. Yin, X. Cao, X. Xie, C. Tan, X. Huang, B. Chen, F. Chen, Q. Yang, X. Bu, X. Lu, L. Sun, H. Zhang, *Adv. Mater.* **2013**, *25*, 5916.
- [16] H. W. Liang, Q. F. Guan, L. F. Chen, Z. Zhu, W. J. Zhang, S. H. Yu, *Angew. Chem., Int. Ed. Engl.* **2012**, *51*, 5101.
- [17] X. Zhao, L. Li, B. Li, J. Zhang, A. Wang, *J. Mater. Chem. A* **2014**, *2*, 18281.
- [18] R. Du, N. Zhang, H. Xu, N. Mao, W. Duan, J. Wang, Q. Zhao, Z. Liu, J. Zhang, *Adv. Mater.* **2014**, *26*, 8053.
- [19] X. Gui, J. Wei, K. Wang, A. Cao, H. Zhu, Y. Jia, Q. Shu, D. Wu, *Adv. Mater.* **2010**, *22*, 617.
- [20] H. Bi, X. Huang, X. Wu, X. Cao, C. Tan, Z. Yin, X. Lu, L. Sun, H. Zhang, *Small* **2014**, *10*, 3544.
- [21] Y. Gao, Y. S. Zhou, W. Xiong, M. Wang, L. Fan, H. Rabiee-Golgir, L. Jiang, W. Hou, X. Huang, L. Jiang, J. F. Silvain, Y. F. Lu, *ACS Appl. Mater. Interfaces* **2014**, *6*, 5924.
- [22] M. Kettunen, R. J. Silvennoinen, N. Houbenov, A. Nykänen, J. Ruokolainen, J. Sainio, V. Pore, M. Kemell, M. Ankerfors, T. Lindström, M. Ritala, R. H. A. Ras, O. Ikkala, *Adv. Funct. Mater.* **2011**, *21*, 510.
- [23] Z. Cheng, J. Wang, H. Lai, Y. Du, R. Hou, C. Li, N. Zhang, K. Sun, *Langmuir* **2015**, *31*, 1393.
- [24] T. Sun, G. Wang, L. Feng, B. Liu, Y. Ma, L. Jiang, D. Zhu, *Angew. Chem. Int. Ed. Engl.* **2004**, *43*, 357.
- [25] J. W. Wang, B. D. Mao, J. L. Gole, C. Burda, *Nanoscale* **2010**, *2*, 2257.
- [26] H. Bi, X. Xie, K. Yin, Y. Zhou, S. Wan, L. He, F. Xu, F. Banhart, L. Sun, R. S. Ruoff, *Adv. Funct. Mater.* **2012**, *22*, 4421.
- [27] H. Zhu, D. Chen, W. An, N. Li, Q. Xu, H. Li, J. He, J. Lu, *Small* **2015**, *11*, 5222.
- [28] H. Sun, Z. Xu, C. Gao, *Adv. Mater.* **2013**, *25*, 2554.
- [29] W. Liu, Y. Wang, Z. Li, *Chem. Commun.* **2014**, *50*, 10311.
- [30] C. Chen, R. Li, L. Xu, D. Yan, *RSC Adv.* **2014**, *4*, 17393.
- [31] H. Zhu, D. Chen, N. Li, Q. Xu, H. Li, J. He, J. Lu, *Adv. Funct. Mater.* **2015**, *25*, 597.
- [32] Z. Li, Y. Wang, A. Kozbial, G. Shenoy, F. Zhou, R. McGinley, P. Ireland, B. Morganstein, A. Kunkel, S. P. Surwade, L. Li, H. Liu, *Nat Mater.* **2013**, *12*, 925.
- [33] J. Rafiee, M. A. Rafiee, Z. Z. Yu, N. Koratkar, *Adv. Mater.* **2010**, *22*, 2151.
- [34] Y. Wu, N. Yi, L. Huang, T. Zhang, S. Fang, H. Chang, N. Li, J. Oh, J. A. Lee, M. Kozlov, A. C. Chipara, H. Terrones, P. Xiao, G. Long, Y. Huang, F. Zhang, L. Zhang, X. Lepro, C. Haines, M. D. Lima, N. P. Lopez, L. P. Rajukumar, A. L. Elias, S. Feng, S. J. Kim, N. T. Narayanan, P. M. Ajayan, M. Terrones, A. Aliev, P. Chu, Z. Zhang, R. H. Baughman, Y. Chen, *Nat. Commun.* **2015**, *6*, 6141.
- [35] W. Gao, G. Wu, M. T. Janicke, D. A. Cullen, R. Mukundan, J. K. Baldwin, E. L. Brosha, C. Galande, P. M. Ajayan, K. L. More, A. M. Dattelbaum, P. Zelenay, *Angew. Chem. Int. Ed. Engl.* **2014**, *53*, 3588.
- [36] F. Cataldo, *J. Nanosci. Nanotechnol.* **2007**, *7*, 1446.
- [37] S. Huh, J. Park, Y. S. Kim, K. S. Kim, B. H. Hong, J.-M. Nam, *ACS Nano* **2011**, *5*, 9799.
- [38] R. Wang, K. Hashimoto, A. Fujishima, M. Chikuni, E. Kojima, A. Kitamura, M. Shimohigoshi, T. Watanabe, *Nature* **1997**, *388*, 431.
- [39] L. Zhang, J. Liang, Y. Huang, Y. Ma, Y. Wang, Y. Chen, *Carbon* **2009**, *47*, 3365.